Could an increase in airway smooth muscle shortening velocity cause airway hyperresponsiveness?

Sharon R. Bullimore, Sana Siddiqui, Graham M. Donovan, James G. Martin, James Sneyd, Jason H. T. Bates and Anne-Marie Lauzon

Am J Physiol Lung Cell Mol Physiol 300:L121-L131, 2011. First published 22 October 2010; doi:10.1152/ajplung.00228.2010

Am J Physiol Lung Cell Mol Physiol 300: L121–L131, 2011.
First published October 22, 2010; doi:10.1152/ajplung.00228.2010.

Could an increase in airway smooth muscle shortening velocity cause airway hyperresponsiveness?

Sharon R. Bullimore,[1] Sana Siddiqui,[1] Graham M. Donovan,[2] James G. Martin,[1] James Sneyd,[2] Jason H. T. Bates,[3] and Anne-Marie Lauzon[1]

[1]*Meakins-Christie Laboratories, McGill University, Montreal, Quebec, Canada;* [2]*Department of Mathematics, University of Auckland, Auckland, New Zealand; and* [3]*Vermont Lung Center, University of Vermont College of Medicine, Burlington, Vermont*

Submitted 8 July 2010; accepted in final form 19 October 2010

Bullimore SR, Siddiqui S, Donovan GM, Martin JG, Sneyd J, Bates JH, Lauzon A. Could an increase in airway smooth muscle shortening velocity cause airway hyperresponsiveness? *Am J Physiol Lung Cell Mol Physiol* 300: L121–L131, 2011. First published October 22, 2010; doi:10.1152/ajplung.00228.2010.—Airway hyperresponsiveness (AHR) is a characteristic feature of asthma. It has been proposed that an increase in the shortening velocity of airway smooth muscle (ASM) could contribute to AHR. To address this possibility, we tested whether an increase in the isotonic shortening velocity of ASM is associated with an increase in the rate and total amount of shortening when ASM is subjected to an oscillating load, as occurs during breathing. Experiments were performed in vitro using 27 rat tracheal ASM strips supramaximally stimulated with methacholine. Isotonic velocity at 20% isometric force (Fiso) was measured, and then the load on the muscle was varied sinusoidally (0.33 ± 0.25 Fiso, 1.2 Hz) for 20 min, while muscle length was measured. A large amplitude oscillation was applied every 4 min to simulate a deep breath. We found that: *1*) ASM strips with a higher isotonic velocity shortened more quickly during the force oscillations, both initially ($P < 0.001$) and after the simulated deep breaths ($P = 0.002$); *2*) ASM strips with a higher isotonic velocity exhibited a greater total shortening during the force oscillation protocol ($P < 0.005$); and *3*) the effect of an increase in isotonic velocity was at least comparable in magnitude to the effect of a proportional increase in ASM force-generating capacity. A cross-bridge model showed that an increase in the total amount of shortening with increased isotonic velocity could be explained by a change in either the cycling rate of phosphorylated cross bridges or the rate of myosin light chain phosphorylation. We conclude that, if asthma involves an increase in ASM velocity, this could be an important factor in the associated AHR.

trachealis; cross-bridge model; latchbridge; deep inspiration; oscillation

ONE OF THE DEFINING FEATURES of asthma is airway hyperresponsiveness (AHR), an increase in the magnitude and/or sensitivity of the response to bronchoconstricting stimuli. Many factors have been identified that could contribute to AHR, including an increase in the capacity of airway smooth muscle (ASM) to generate force, airway wall thickening, alterations in the mechanical properties of the lung parenchyma or the airway wall, and abnormal neural control (5). It has also been suggested that an increase in the shortening velocity of ASM could cause AHR (2, 31, 41). This has been proposed based on two lines of evidence. First, in vivo studies have shown that the airways of both normal and asthmatic subjects dilate transiently when a deep inspiration is taken during induced bronchoconstriction, but that the subsequent reconstriction is more rapid in asthmatics (23, 25, 35). Second, in vitro measurements have shown that bronchial ASM cells taken from asthmatic patients have an increased shortening velocity relative to controls (29) as do human bronchial ASM sensitized in vitro (32), ASM from animal models of allergic AHR (2, 11, 31, 43), and ASM from animals with innate AHR (6, 9, 10, 44, 46).

It is not immediately obvious why an increase in ASM shortening velocity should result in AHR. AHR is a reflection of an abnormal degree of airway narrowing, which is primarily a function of the final length to which the ASM shortens, rather than the rate of shortening. One possibility that has been suggested is that an increase in ASM shortening velocity could increase the total amount that stimulated ASM shortens during breathing by increasing the amount by which it can shorten during the expiratory phase or pause of each breath (41). This has not yet been convincingly demonstrated experimentally, however.

Another factor that makes it difficult to determine the implications of an increase in shortening velocity is that in vitro measurements of velocity are typically made under constant force (isotonic) conditions, whereas ASM in vivo is continually subjected to cyclic stretch and shortening due to breathing. It is well established that the relationships between muscle force, length, and velocity are very different under isotonic and cyclic loading conditions (4, 14, 15, 17, 38, 39). Therefore, it is unclear whether an increase in shortening velocity measured under isotonic conditions will translate into an increase in the rate of shortening during breathing. The role played by ASM shortening velocity in AHR thus remains unclear despite the compelling experimental data hinting at its importance, so elucidating the nature of this role continues to be an important problem.

To investigate the general question of whether an increase in the shortening velocity of ASM could contribute to AHR, we addressed the following three specific experimental questions: *1*) Is there an association between the isotonic shortening velocity of ASM and the rate at which it shortens when subjected to an oscillating load? *2*) Is there an association between the isotonic shortening velocity of ASM and the total amount that it shortens when subjected to an oscillating load? *3*) If the answer to *question 2* is yes, how does the magnitude of this effect compare to the effect of an increase in the force-generating capacity of the muscle? These questions were addressed by performing in vitro mechanical tests on rat tracheal ASM strips. We also investigated possible mechanisms underlying our experimental observations us-

Address for reprint requests and other correspondence: A. Lauzon, Meakins-Christie Laboratories, McGill Univ., 3626 St. Urbain St., Montreal, QC, Canada H2X 2P2 (e-mail: anne-marie.lauzon@mcgill.ca).

ing a four-state cross-bridge model similar to that of Mijailovich et al. (30).

METHODS

Experimental Methods

All procedures were approved by the McGill University Animal Care Committee and complied with the guidelines of the Canadian Council on Animal Care.

Animals. The experiments were performed using tracheal ASM strips from 27 rats (age: 8–13 wk; mass: 175–290 g) comprising 6 Fischer rats (Harlan USA and Charles River, Canada), 10 Lewis rats (Harlan USA and Charles River, Canada), and 11 Brown Norway rats (ssNOlaHsd, Harlan UK). Seven of the Brown Norway rats were subjected to a 4-wk allergen sensitization and challenge protocol that has been shown to induce AHR (40). They were sensitized to ovalbumin using a single intraperitoneal injection, and then the test animals ($n = 3$) were challenged three times intratracheally at 5-day intervals with aerosolized ovalbumin while the control animals ($n = 4$) were challenged with phosphate-buffered saline. Because we did not find systematic differences in ASM velocity between the different groups of rats, we pooled all the data.

Preparation of muscle strips. One muscle strip from each animal was tested. The rats were euthanized by intraperitoneal injection of an overdose of pentobarbital sodium. Tracheae were dissected out and placed in calcium-free Krebs-Henseleit (KH) solution to minimize intrinsic tone (composition in mM: 118.0 NaCl, 4.5 KCl, 2.5 $MgSO_4$, 1.2 KH_2PO_4, 25.5 $NaHCO_3$, 10.0 glucose, pH 7.4; aerated with 95% O_2/5% CO_2 for at least 30 min). Loose connective tissue was removed from the trachea, and it was cut transversely to separate out a single cartilage ring with adjoining muscle tissue. The properties of tracheal smooth muscle vary along the length of the trachea (12), so we standardized the sites from which the rings were obtained. In Fischer and Lewis rats, rings from the central third of the trachea were used. In Brown Norway rats, rings from the caudal third were used, as these animals had been intubated and we wanted to avoid tissue that might have come into contact with the intratracheal tube.

The tracheal rings were cut on either side of the smooth muscle to obtain muscle strips with 1–2 mm of cartilage at either end. Round-ended forceps were rubbed gently over the epithelial surface of the muscle and cartilage to remove the epithelium, and T-shaped aluminum foil clips were wrapped around the cartilage at the ends of the strips to allow them to be attached to the experimental apparatus.

Experimental apparatus. The muscle strips were mounted horizontally in an experimental chamber. They were attached at one end to a length controller (model 322C-I; Aurora Scientific, Ontario, Canada) and at the other end to a force transducer (model 404A, Aurora Scientific). Computer software (model 600A, Aurora Scientific) controlled muscle strip length and recorded force. In force control mode, which was used for the force oscillation protocol and to measure isotonic shortening velocity, the computer varied muscle strip length to achieve a specified target force. KH solution, aerated with 95% O_2/5% CO_2, was circulated through the experimental chamber at ~6.5 ml/min. A water jacket maintained the chamber at 37°C.

Experimental procedure. In each muscle strip, we measured both the isotonic shortening velocity and the rate and degree of shortening in response to a force oscillation protocol. The force oscillation protocol was based on the approach of Fredberg et al. (15) but differed in that the oscillations began following an isometric contraction, rather than following a period of isotonic shortening. An example of force and length data recorded during these measurements is shown in Fig. 1.

The muscle strips were initially mounted in calcium-free KH solution to suppress basal tone. Length was set to a reference length (L_{ref}), which was defined as 1.25× unstretched length. L_{ref} was defined relative to unstretched length rather than in situ length because we found that this gave us much more repeatable results with these small tissue strips. Throughout the rest of the experiment, KH solution containing calcium (2.5 mM $CaCl_2$) was used. The muscle strips were equilibrated for 1 h during which they were stimulated electrically (5-ms square wave pulses, 50 V, 60 Hz) for 10 s every 5 min. Muscle strip length and width at L_{ref} were measured twice during the experiment using a microscope with an eyepiece reticule, and the two values were averaged. L_{ref} was 0.87–1.80 mm and width was 0.35–0.82 mm.

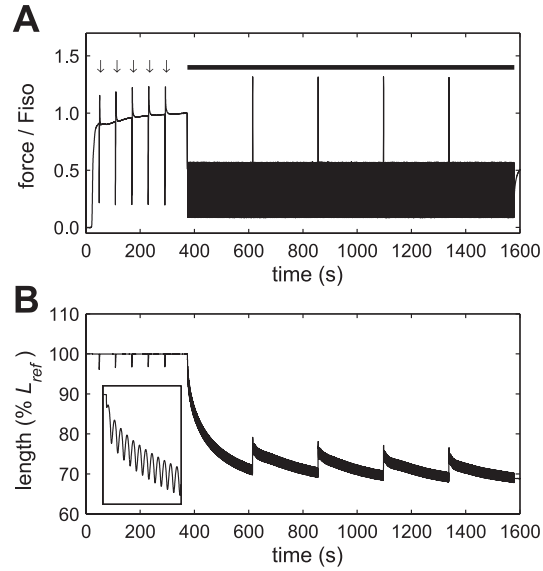

Fig. 1. Example of raw force (*A*) and length (*B*) data obtained during the isotonic clamps (arrows in *A*) and force oscillation protocol (thick bar in *A*). Methacholine stimulation began at ~20 s. Five 120-ms force clamps at 20% isometric force (Fiso) were performed at 1-min intervals before the force oscillation protocol began 6 min into activation. Force in the figure is expressed relative to Fiso at the start of the force oscillation protocol, but the force during each clamp was set relative to the current value of Fiso. *Inset* in *B* shows the first 10 s of the force oscillation protocol to illustrate the initial rapid shortening.

Each muscle strip underwent three periods of stimulation with methacholine (MCh; acetyl-β-methylcholine chloride, Sigma Chemical) separated by 10- to 20-min washout periods which allowed complete relaxation. A supramaximal concentration of MCh (5×10^{-4} M) was used throughout. During the second period of stimulation, various velocity measurements were made that were not used. During the third period of MCh stimulation, five force clamps at 20% isometric force (Fiso) were performed at 1-min intervals, beginning ~30 s into activation, to allow isotonic velocity to be measured. The force oscillation protocol began after 6 min of activation. Force was varied sinusoidally (0.33 ± 0.25 Fiso, 1.2 Hz) for 20 min while length was measured. Every 4 min, a larger force oscillation (half sinusoid, 0.4 Hz, peak force: 1.33 Fiso) was applied to simulate a deep breath. Fiso was measured immediately before each force clamp, and the force oscillation protocol and force was always normalized to the most recently measured value.

Ten of the muscle strips were used in experiments to determine the effect of an increase in the force-generating capacity of the muscle. This was simulated by decreasing the forces applied during the force oscillation protocol, based on the following reasoning: If an increase in the force-generating capacity of ASM occurs due to an increase in the number of muscle cells acting in parallel, without any change in the properties of individual cells, then the loads applied to the muscle will be shared between a greater number of cells and so will be a lower proportion of the maximum isometric force of each cell. Therefore, for individual cells, a decrease in applied load is equivalent to an increase in muscle strength.

All 10 strips were subjected to the force oscillation protocol twice, once using 100% of the forces stated above and once with the forces multiplied by a factor, a, of 0.5, 0.6, 0.7, 0.8, or 0.9. Between the two force oscillation protocols there was a recovery period during which the muscle strips were relaxed, stretched back to L_{ref}, equilibrated for 75 min with electrical field stimulation, and then stimulated twice for 6 min with MCh. During the following period of MCh stimulation, five force clamps at 0.2 Fiso were performed, followed by the second force oscillation protocol. In preliminary experiments, we observed an order effect, in that muscle strips that were subjected twice to the 100% force condition tended to shorten less on the second occasion. To account for this, two strips were tested for each value of a, one undergoing the 100% force condition first and the other undergoing the reduced force condition first, and the results for the two strips were averaged.

Data analysis. Shortening velocity during the isotonic force clamps was determined by fitting a straight line to the relationship of length to time between 65 and 115 ms after the start of the force clamp, and dividing the slope of the line by L_{ref}. The velocities measured during the five force clamps were extrapolated forward to predict isotonic velocity at the start of the force oscillation protocol using a power-law relationship of the form $v = kt^b$, where v is velocity at 0.2 Fiso, t is time, and k and b are constants. Relationships between this predicted isotonic velocity and the response of the muscle strips to the force oscillation protocol were determined by linear regression analysis in Matlab (The Mathworks). The percentage increase in force-generating capacity that was simulated by multiplying the applied forces by a was calculated as $100 \cdot (1/a) - 1]$. The percentage increase in the total amount of shortening in the reduced force condition compared with the 100% force condition was calculated for each muscle strip and then averaged within each pair of strips that were tested with the same value of a. $P < 0.05$ was considered significant.

Modeling Methods

The model. We used a four-state, cross-bridge model based on that of Mijailovich et al. (30). This model combines Hai and Murphy's latch-bridge model of isometric contractions in smooth muscle (19) with Huxley's cross-bridge model (22), which can model dynamic as well as isometric contractions. These two models have also been combined by Hai and Murphy (20) and Yu et al. (48), but we chose to adopt the approach of Mijailovich et al. because these authors obtained complete solutions to the four-state model, whereas the authors of the previous studies reduced the four-state model to an equivalent two-state model and either solved the equations using an approximation (48) or considered only the steady-state solutions (20). The major differences between our model and that of Mijailovich et al. (30) were as follows: *1*) We added a length-tension relationship because we found that this was necessary to prevent the model from shortening indefinitely when simulating the force oscillation protocol. This was implemented by multiplying the force predicted by the cross-bridge model by a factor between 0 and 1 depending on the current length. *2*) We developed an algorithm that allowed us to specify force and predict velocity, whereas cross-bridge models typically operate in the opposite fashion. *3*) We used higher rate constants for cross-bridge attachment and detachment, as explained below. *4*) We normalized force to the isometric force predicted for the rate constants that we used, rather than to the isometric force corresponding to 100% phosphorylation. *5*) We did not use the modification of Piazzesi and Lombardi (36), which accounts for actin binding sites being close together. Instead, for simplicity, we assumed, as in the original Huxley model, that the distance between binding sites is large compared with the region over which attachment can occur. When we used the same parameter values and method of force normalization as Mijailovich et al. (30), our simulated force-length loops were very similar to their Fig. 6, suggesting that the influence of this modification was small.

As in the model of Mijailovich et al. (30), myosin heads could be in four different states: dephosphorylated and detached (M), phosphorylated and detached (Mp), phosphorylated and attached (AMp), or dephosphorylated and attached (AM, also known as "latch-bridges"). The rate constants for phosphorylation (k_1) and dephosphorylation (k_2) were the same for attached and detached myosin heads, and latch-bridges detached much more slowly than phosphorylated cross-bridges. The rates at which myosin heads attached to and detached from actin were functions of x, the distance between the equilibrium position of the myosin head and its nearest actin binding site. The maximum value of x at which a myosin head could attach was denoted h, and x was expressed in units of h. The force generated by an attached cross-bridge was proportional to x and was the same for phosphorylated cross-bridges and latch-bridges.

We did not include any passive elements in the model. While such elements are undoubtedly important for the mechanics of ASM (4), as a first approach to modeling our data, our goal was to determine how much of the observed behavior could potentially be due to cross-bridge mechanics. The model equations and method of numerical integration are described in APPENDIX A.

Choice of model parameters. The four states and five rate constants of the model are illustrated in Fig. 2. We used the same forms of the attachment rate function [$f_p(x)$], the detachment rate function for phosphorylated cross-bridges [$g_p(x)$], and the detachment rate function for latch-bridges [$g(x)$] as Mijailovich et al. (30) except that we defined an additional constant, g_{p1s}, so that the detachment rates for isometric contractions and stretch could be varied independently for phosphorylated cross-bridges. Therefore the rate functions were:

$$f_p(x) = \begin{cases} 0 & x < 0 \\ f_{p1}x & 0 \le x \le 1 \\ 0 & x > 1 \end{cases}$$

$$g_p(x) = \begin{cases} g_{p2} & x < 0 \\ g_{p1}x & 0 \le x \le 1 \\ (g_{p1s} + g_{p3})x & x > 1 \end{cases}$$

$$g(x) = \begin{cases} g_2 & x < 0 \\ g_1 x & 0 \le x \le 1 \\ (g_1 + g_3)x & x > 1 \end{cases}$$

where x is in units of h and f_{p1}, g_{p2}, g_{p1}, g_{p1s}, g_{p3}, g_2, g_1, and g_3 are constants.

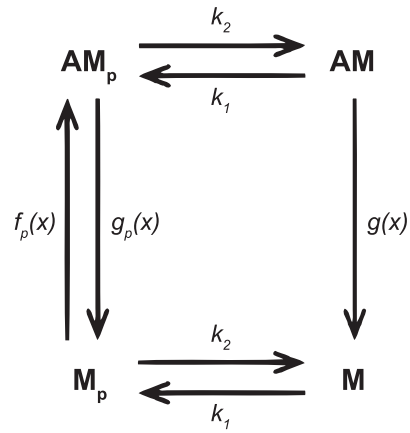

Fig. 2. Model schematic. Myosin heads could be in 4 different states: dephosphorylated and detached (M), phosphorylated and detached (Mp), phosphorylated and attached (AMp), or dephosphorylated and attached (AM). The rate constants for phosphorylation (k_1) and dephosphorylation (k_2) were the same for attached and detached myosin heads. The rate constants for attachment (f_p) and detachment (g_p) of phosphorylated myosin, and detachment of dephosphorylated myosin (g) were functions of myosin strain (x).

When we used the same parameter values that Mijailovich et al. (30) used to model bovine trachealis, the isotonic shortening velocity predicted for 0.2 Fiso was 0.006 L_{ref}/s, which was much lower than the velocities we measured in rat trachealis (0.048–0.065 L_{ref}/s). To overcome this, we increased all myosin attachment and detachment rate constants 4.5× while leaving the phosphorylation (k_1) and dephosphorylation (k_2) rate constants and the scale factor for lengths and velocities ($1h = 0.04\ L_{ref}$) unchanged. This gave a predicted isotonic velocity at 0.2 Fiso of 0.045 L_{ref}/s, which is just below the range of measured values. The parameter values used were (s^{-1}): $f_{p1} = 3.96$, $g_{p1} = 0.99$, $g_{p1s} = 0.99$, $g_{p2} = 19.8$, $g_{p3} = 2.97$, $g_1 = 0.045$, $g_2 = 0.9$, and $g_3 = 0.135$, $k_1 = 0.35$ ($t \leq 5$ s), $k_1 = 0.06$ ($t > 5$ s), $k_2 = 0.1$. The simulation performed using these parameters is referred to as the "baseline" simulation.

To verify that model with the above rate constants could predict the response of rat trachealis to dynamic loading at physiological amplitudes and frequency, we compared model simulations to our previous experimental measurements of the response to length oscillations at 2 Hz (4). We found that the model provided excellent predictions of the effect of oscillation amplitude on mean force and stiffness (Supplemental Fig. S1; Supplemental Material for this article is available online at the Journal website), although, as noted previously (30), the model does not predict the "banana" shape of the loops. By contrast, preliminary tests demonstrated that forces predicted using Huxley's two-state cross-bridge model (22) were much higher than the experimental values. Supplemental Fig. S1 also illustrates the effect of the addition of a length-tension relationship to the model.

We modeled the effects of two factors that could cause an increase in the isotonic shortening velocity of ASM. The first factor was an increase in the attachment and detachment rates of the phosphorylated cross-bridges. This simulates an increase in the ratio of the +insert to the −insert isoform of myosin since, relative to the −insert, the +insert isoform has a higher detachment rate and propels actin at a higher velocity but generates the same unitary and average force (27). The rate constants used were (s^{-1}): $f_{p1} = 9.11$, $g_{p1} = 2.28$, $g_{p2} = 45.54$. These values were chosen by keeping f_{p1}, g_{p1}, and g_{p2} in the ratios used by Mijailovich et al. (30) and increasing them until the isotonic velocity at 0.2 Fiso was 50% greater than for the baseline parameter values (i.e., 0.0675 L_{ref}/s, which was just above the range of measured values). The detachment rates of the latch-bridges [$g(x)$] and of the phosphorylated cross-bridges during stretch (g_{p1s} and g_{p3}) were not altered. This change increased isotonic shortening velocity without altering Fiso or the rate of isometric force development.

The second factor we investigated for altering shortening velocity in the model was to increase the phosphorylation rate constant (k_1) to simulate an increase in myosin light chain kinase activity. This resulted in an increase in the ratio of phosphorylated cross-bridges to latch-bridges and also in the rate of isometric force rise and Fiso. We accounted for the latter effect by normalizing all applied forces to Fiso, as in the experiments. The values of k_1 used were (s^{-1}): 1.08 for $t \leq 5$ s and 0.185 for $t > 5$ s. These values were obtained by increasing k_1 until the isotonic velocity at 0.2 Fiso was 50% higher than for the baseline parameter values.

Simulating the force oscillation protocol. The simulations began with all the myosin heads detached and unphosphorylated. A 6-min isometric contraction was simulated before the force oscillation protocol, to match the experiments. Cross-bridge models usually take velocity as an input and predict force, but, to model the force oscillation protocol, we needed to be able to specify a target force and predict velocity. The algorithm that we used to do this is described in APPENDIX B.

The target forces that were used to simulate the low-amplitude force oscillations were the same as those used in the experiments, i.e., a sine wave with mean force of 0.33 Fiso, amplitude ± 0.25 Fiso, and frequency 1.2 Hz. However, we found that, when the model parameters were set as described above, the simulations were unable to generate forces as high as those applied during the deep breaths. This is not surprising, as mean force in the model decreases as oscillation amplitude increases (30) and suggests that most of the force during the deep breaths in the experiments was due to passive elements. To overcome this, we applied a much smaller and quicker deep breath to the model (half sinusoid, peak force: 0.83 Fiso, freq: 1.6 Hz). This generated a stretch that was of similar magnitude to the stretch generated by the deep breaths in the experiments and therefore allowed us to investigate the behavior of the model following a length perturbation matching that in the experiments. We simulated an increase in the force-generating capacity of the muscle using the same method as in the experiments, i.e., by multiplying the target forces (including the deep breaths) by a factor of 0.5 or 0.67 to simulate a 100% or 50% increase in force-generating capacity, respectively.

Various length-tension relationships were used. These are discussed in more depth in the RESULTS and DISCUSSION sections. They were implemented by multiplying the force predicted by the cross-bridge model (APPENDIX A) by a factor between 0 and 1 according to the current length. This was intended to reflect the influence of factors such as internal load and a decrease in the overlap between actin and myosin filaments.

RESULTS

Experimental Results

Question 1: Is there an association between the isotonic shortening velocity of ASM and the rate at which it shortens when subjected to an oscillating load? Examples of the response to the force oscillation protocol in two muscle strips with different isotonic velocities are shown in Fig. 3*A*. To determine the initial rate of shortening, we calculated the mean rate of shortening between 1 and 26 s after the start of the protocol. The first 1 s was excluded because the initial phase of shortening was very rapid and was assumed to be due to elastic recoil (Fig. 1*B*, *inset*). This time period was chosen because ~40–50% of the total shortening observed during the force oscillation protocol occurred within the first 26 s. The mean velocity during this initial period of the protocol increased as isotonic velocity increased ($P < 0.001$, Fig. 3*B*), indicating that the answer to *Question 1* is yes.

To determine whether this increase in the initial rate of shortening during force oscillations was due to an increase in shortening per cycle, or a decrease in stretch per cycle, we also calculated the mean stretch and mean shortening per cycle between 1 and 26 s of the force oscillation protocol. Neither parameter was significantly related to isotonic velocity, however, indicating that the initial rate of shortening was a function of the balance between the amounts of stretch and shortening per cycle, rather than being governed by one or other of these variables.

To determine the mean rate at which the muscle strips reshortened after the deep breaths, we fitted straight lines to the length-time data over the 4-min period after each deep breath and averaged the slopes of the four lines calculated for each muscle strip. We found that the mean rate of shortening after the deep breaths also increased as isotonic velocity increased (Fig. 3*C*, $P = 0.002$).

It is interesting to note that the initial shortening velocity during the force oscillation protocol was much greater than the velocity of reshortening between deep breaths (Fig. 3, *B* and *C*). We found that shortening velocity was predominantly a function of muscle strip length (Supplemental Fig. S2). Therefore, this difference in velocity can be explained by the shorter muscle length during reshortening.

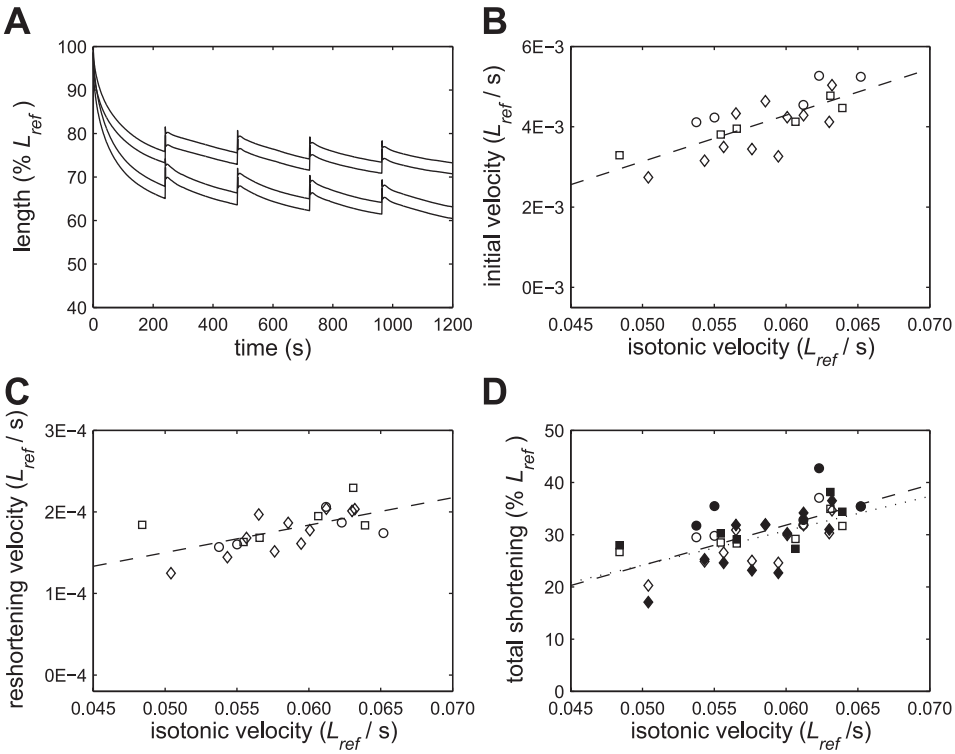

Fig. 3. *A*: examples of responses to the force oscillation protocol in 2 muscle strips with isotonic velocities at 0.2 Fiso of 0.048 L_{ref}/s and 0.063 L_{ref}/s. The lines shown pass through the maxima and minima of each oscillation cycle. As observed overall, the strip with the higher isotonic shortening velocity shortened further. *B*: muscle strips with higher isotonic velocities shortened more quickly during the initial phase of the force oscillation protocol ($P < 0.001$). *C*: the magnitude of the mean velocity of reshortening after the deep breaths increased as isotonic velocity increased ($P = 0.002$). *D*: the total amount that the muscle strips shortened during the force oscillation protocol, both before the first deep breath (open symbols, dotted line) and by the end of the protocol (filled symbols, dashed line), increased as isotonic velocity increased ($P < 0.005$). Squares, Lewis rats; circles, Fischer rats; diamonds, Brown Norway rats.

Question 2: Is there an association between the isotonic shortening velocity of ASM and the total amount that it shortens when subjected to an oscillating load? There was a highly significant relationship between the isotonic shortening velocity of a muscle strip and the total amount by which it shortened during the force oscillation protocol (Fig. 3*D*), such that an increase in shortening velocity was associated with an increase in the total amount of shortening both before the first deep breath ($P < 0.001$) and by the end of the protocol ($P = 0.004$). This relationship remained significant even when the two data points corresponding to the least and the greatest amount of shortening were excluded from the analysis ($P = 0.001$ for shortening before the first deep breath; $P = 0.037$ for shortening by the end of the protocol). Therefore, the answer to *Question 2* is yes.

Question 3: How does the magnitude of the effect of an increase in velocity compare to the effect of an increase in the force-generating capacity of the muscle? When an increase in force-generating capacity was simulated by decreasing the forces applied during the force oscillation protocol by multiplying them by 0.5, 0.6, 0.7, 0.8, or 0.9, the total amount by which the muscle strips shortened, both before the first deep breath ($P = 0.005$) and by the end of the protocol ($P = 0.02$), increased. These data are shown in Fig. 4 expressed in terms of percentage increase in shortening against percentage increase in force-generating capacity. The regression lines have been forced through the origin to reflect the fact that zero increase in force should correspond to zero increase in shortening. The 95% confidence intervals for the slopes of the regression lines were 0.44–0.70 for shortening before the first deep breath and 0.47–1.00 for shortening by the end of the protocol. Both these slopes were significantly less than 1, indicating that the proportional increase in shortening was less than the proportional increase in force-generating capacity.

To compare the magnitude of the effect of an increase in velocity with the effect of an increase in force-generating capacity, the velocity data were expressed as percentage changes in velocity and total shortening. Because the choice of the value relative to which the percentages were calculated was arbitrary, we tested the effect of using two different points on the regression lines in Fig. 3*D*, corresponding to the minimum and maximum measured velocities. To determine the magnitude of the effect of velocity, we plotted percent increase in shortening against percent increase in velocity, fitted regression lines through the origin, and compared the slopes of these lines to the slopes of the lines for force-generating capacity. When percentages were calculated relative to the minimum

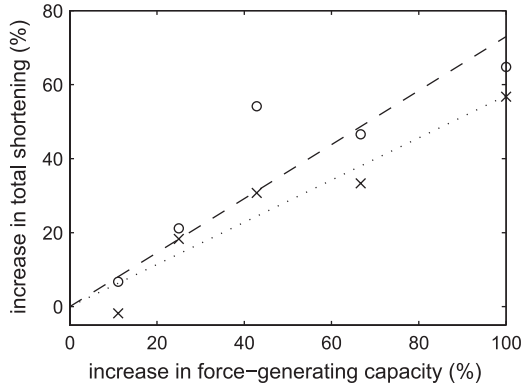

Fig. 4. Effect of an increase in the force-generating capacity of the muscle on the total amount by which the muscle strips shortened during the force oscillation protocol, both before the first deep breath (×, dotted line) and by the end of the protocol (○, dashed line). The regression lines have been forced through the origin. An increase in force-generating capacity was simulated by reducing the applied forces by multiplying them by a factor between 0.5 and 0.9.

velocity reference point, the slopes of the relationships were significantly greater than 1 and significantly greater than the slopes for force-generating capacity. However, when percentages were calculated relative to the maximum velocity reference point, although the calculated slopes were greater than 1, the 95% confidence intervals included 1 and the confidence interval for shortening at the end of the protocol overlapped slightly with the confidence interval for force-generating capacity. Therefore, we can conclude that the effect of an increase in isotonic velocity is equal to or greater than the effect of an increase in force-generating capacity.

Modeling Results

Modeling the length-time behavior during the force oscillation protocol. Our goal was to determine whether the experimentally observed effects of an increase in velocity could be reproduced by a cross-bridge model, so we used the model to address the same three questions that were addressed experimentally. Before doing this, however, we tested whether the shape of the experimentally observed relationship of length to time (Fig. 3*A*) could be reproduced by altering the length-tension relationship used in the model. We initially used a linear length-tension relationship (LTR1; Fig. 5*A*) that was similar to the isometric length-tension relationship that has been measured experimentally (42). With this length-tension relationship, the simulations shortened rapidly until they reached an equilibrium length at which there was no net change in length, and then quickly returned to this length after each deep breath (Fig. 5*B*, *simulation 1*). This behavior is very different from the behavior observed experimentally in which shortening velocity began to decrease after the first oscillation cycle and continued to decrease at a diminishing rate (Figs. 3*A* and S2).

We were able to reproduce behavior similar to the experimentally observed behavior by using LTR2 (Fig. 5*A*). The shape of this relationship was derived from the shape of the observed velocity-length relationship (Supplemental Fig. S2). A simulation obtained with LTR2 is shown in Fig. 5*B* (*simulation 2*) and is very similar in nature to the experimental data. We found, however, that this length-tension relationship could not be used to predict the effects of changes in isotonic shortening velocity or force-generating capacity because it was so shallow that the muscle would quickly shorten to zero length if its capacity to shorten were increased. This implies that the effective length-tension relationship during shortening is different under different loading conditions. However, we did not want to invoke different length-tension relationships in each simulation, simply to achieve a good fit to each data set.

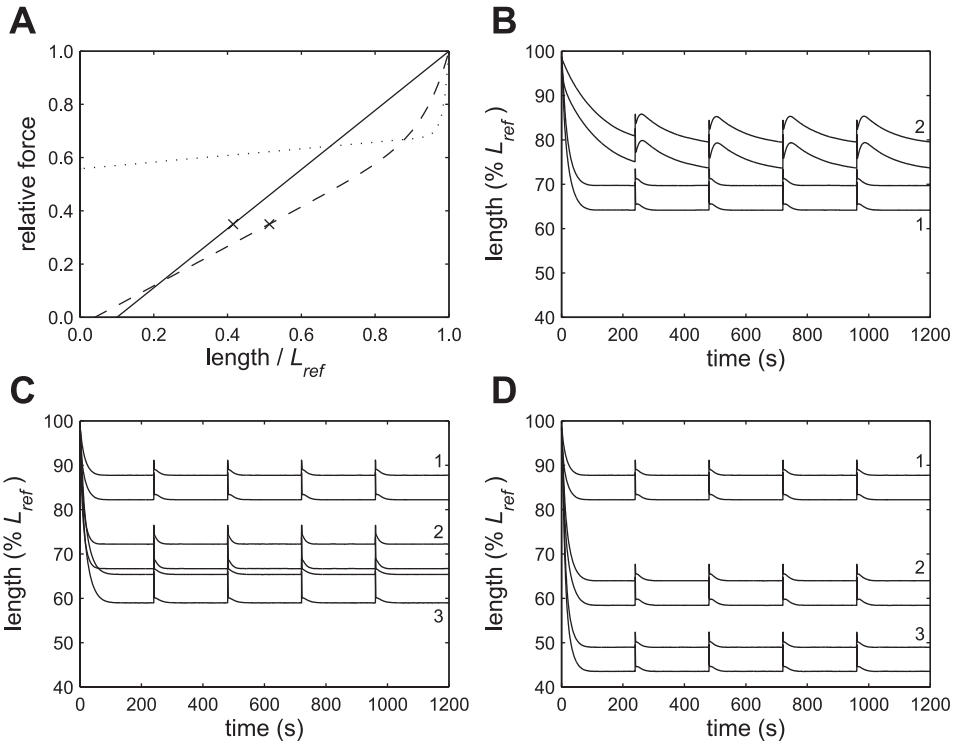

Fig. 5. Model simulations. *A*: length-tension relationships used in the modeling: LTR1 (solid line), LTR2 (dotted), LTR3 (dashed). The crosses indicate the final lengths that would be reached by a simulation that shortened to a relative force of 0.35 on LTR1 or LTR3. LTR2 and LTR3 follow the relationship $F = a\exp(bL) + cL + d$, where F is relative force, L is length/L_{ref}, a, b, c, and d are constants, and a was chosen to ensure the relationship went through (1, 1). For LTR2, $b = 70$, $c = 0.125$, and $d = 0.558$. For LTR3, $b = 15$, $c = 0.74$, and $d = -0.03$. *B*: model simulations performed using different length-tension relationships. The pairs of lines indicate the maxima and minima of each oscillation cycle. When LTR1 was used, the simulation shortened rapidly to a steady-state length and returned to that length after each deep breath (1). A length-time relationship similar to that observed in the experimental data could be reproduced by using LTR2 (2). *C*: predicted effect of a 50% increase in the isotonic shortening velocity at 0.2 Fiso. Simulations were performed using LTR3. When an increase in isotonic velocity was simulated by increasing the cycling rate of the phosphorylated cross-bridges (3) or by increasing the rate of myosin light chain phosphorylation (2), the predicted total shortening was at least double that in the baseline simulation (1). *D*: predicted effect of an increase in force-generating capacity. Simulations were performed using LTR3. When a 50% (2) or 100% (3) increase in force-generating capacity was simulated, the predicted total shortening was much greater than in the baseline simulation (1, same as in *C*).

Therefore, we performed all further simulations using a single length-tension relationship that was a compromise between LTR1 and LTR2 (Fig. 5*A*, LTR3). This length-tension relationship generated behavior that was intermediate between that observed with the other two length-tension relationships (Fig. 5, *C* and *D*). Therefore, the simulations captured some essential elements of the experimental data but exhibited some important differences. We also found that the amplitude of length oscillation in the simulations (Fig. 5) was about twice the measured amplitude (Fig. 3*A*). This may be because parallel passive elements resisted stretch in the tissue strips but were not included in the model.

Question 1: Does an increase in the isotonic velocity of the model cause an increase in the rate of shortening in response to an oscillating load? To answer this question, mean shortening velocity was calculated between 1 and 26 s after the start of the simulations. When a 50% increase in isotonic shortening velocity was modeled by increasing the cycling rate of the phosphorylated cross-bridges by 2.3× or the phosphorylation rate by 3.1×, this initial shortening velocity was increased relative to the baseline simulation by 2.9× and 2.6×, respectively. When phosphorylation rate was increased, the increase in initial shortening velocity was due to both an increase in mean shortening per cycle and a decrease in mean stretch per cycle. However, when the cycling rate of the phosphorylated cross-bridges was increased, both stretch per cycle and shortening per cycle increased, but the increase in the amount of shortening was greater than the increase in the amount of stretch. Therefore, in the model, as in the experiments, the answer to *Question 1* is yes.

Question 2: Does an increase in the isotonic velocity of the model cause an increase in the total amount of shortening in response to an oscillating load? When a 50% increase in isotonic shortening velocity was modeled by increasing the cycling rate of the phosphorylated cross-bridges or the phosphorylation rate, the simulations shortened approximately twice as far before reaching an equilibrium length (Fig. 5*C*). Therefore, in the model, as in the experiments, the answer to *Question 2* is yes.

Question 3: How does the magnitude of the effect of an increase in velocity compare to the effect of an increase in force-generating capacity in the model? When a 50% or 100% increase in force-generating capacity was modeled by decreasing the target forces applied during the simulations, the simulations shortened further and faster than the baseline simulation (Fig. 5*D*). We found that regardless of the length-tension relationship used, a simulation with a given set of rate constants and target forces always shortened to a similar relative force on the length-tension relationship. This is illustrated by the crosses in Fig. 5*A*, which indicate the different final lengths that would be reached by a simulation that shortened to a relative force of 0.35, depending on whether LTR1 or LTR3 was used. Because the amount of shortening, and, therefore, the differences between the simulations depended on the shape of the length-tension relationship, we focused on ranking the amount by which the simulations shortened, rather than considering the magnitude of the differences between them. The model predicted that a 50% increase in force-generating capacity (Fig. 5*D*, *simulation 2*) would result in an amount of shortening that was equal to (Fig. 5*C*, *simulation 3*) or greater than (Fig. 5*C*, *simulation 2*) the amount of shortening when isotonic velocity was increased by 50%. This was somewhat different from what was observed experimentally, where the effect of an increase in velocity was equal to or greater than the effect of an increase in force-generating capacity.

DISCUSSION

Many factors have been identified that could potentially cause AHR, and the relative importance of these factors in asthma remains controversial. It is likely that several factors interact to cause the observed AHR (5). For a long time, it has been known that there is an association between AHR and an increased ASM shortening velocity in animal models (2, 6, 9–11, 31, 43, 44, 46), and this has raised the question of whether an increased ASM velocity could be yet another causative factor in AHR (15, 41). We tackled this question by breaking it down into three subquestions that could be addressed experimentally.

We first showed that ASM that shortens more quickly under isotonic conditions also shortens more quickly when subjected to an oscillating load. This is important for determining whether in vitro measurements of isotonic velocity can predict the behavior of muscle under the dynamic loading conditions associated with breathing. This relationship is by no means certain because the net muscle shortening occurring during breathing depends not only on the rate of ASM shortening during expiration but also on the resistance of the muscle to stretch during inspiration and the effect of stretch on the subsequent shortening phase. It is conceivable, for example, that although a faster muscle might shorten more during expiration, it might also stretch more during inspiration, resulting in no change in the average rate of shortening. We found, however, that there was a strong relationship between isotonic velocity and shortening velocity during the force oscillation protocol such that muscle strips with a higher isotonic velocity shortened more quickly both initially and after each deep breath.

The second question that we addressed was whether a faster muscle also shortens further. This is of key importance to the issue of whether an increase in velocity can cause AHR because airway responsiveness depends on airway resistance, which is a function of the degree, rather than the rate, of ASM shortening. We found that faster muscle strips did shorten further during the force oscillation protocol and were therefore hyperresponsive in the sense that they shortened more for a given load and level of activation.

The third important question was whether the effects of an increase in ASM velocity would be physiologically significant. It is conceivable that an increase in velocity might increase both the rate and degree of shortening of ASM but that this effect would be negligible compared with the influence of other factors. We addressed this question by comparing the effect of a change in velocity to the effect of a simulated change in the force-generating capacity of the muscle. We chose force-generating capacity because asthma is known to be associated with an increase in the amount of ASM (24), which suggests a corresponding increase in force-generating capacity if muscle properties remain unchanged, and because it has been shown that this parameter could substantially influence airway responsiveness (26, 33). We found, somewhat unexpectedly, that the effect of an increase in ASM velocity on the amount of

shortening during the force oscillation protocol was at least comparable to the effect of an increase in ASM force, and probably greater.

Previous studies have found differences in ASM shortening velocity between Fischer and Lewis rats (6, 10, 44, 46) and between animals with experimentally induced allergic AHR and controls (2, 11, 31, 43), but we did not find any systematic differences in ASM velocity between these groups. This may have been because we determined isotonic velocity after several minutes of activation, whereas the differences cited above were measured very early in activation. This is supported by the finding of Stephens et al. (43) that the shortening velocity of ASM from ovalbumin-sensitized dogs was elevated at 2 s but not at 8 s into activation. Our results therefore suggest that the AHR that is observed in Fischer rats (44) and in allergen-sensitized Brown Norway rats (40) is not due to a sustained elevation of ASM shortening velocity.

The force transducer that we used drifted by a small amount (up to 0.21 mN) during the course of each experiment. We considered the possibility that the resulting error in the forces applied during the force clamps and force oscillation protocol might be responsible for the relationships that we observed between isotonic velocity and the rate and amount of shortening during the force oscillation protocol. We found, however, that none of the measured parameters were significantly related to the amount of transducer drift (see Supplemental Fig. S3), indicating that this source of error cannot explain our findings.

We used a cross-bridge model to investigate possible mechanisms underlying the behavior that we observed experimentally. The advantage of the model was that, unlike in the experiments, we were able to test the effect of altering velocity while keeping other aspects of the model constant. By altering the cycling rates of the phosphorylated cross-bridges, we altered isotonic shortening velocity without changing isometric force, latch-bridge properties, or the length-tension relationship. Passive properties were also unchanged in the sense that they were absent. When we altered velocity by changing the rate of myosin light chain phosphorylation, isometric force was also altered, but we were able to account for this by scaling the target forces applied during the simulations. When isotonic velocity in the model was increased by either of the above methods, we found that, as in the experiments, not only the rate but also the amount of shortening in response to the force oscillation protocol was increased. The reason for this was that the model simulations shortened until they reached a relative force on the length-tension relationship at which the amount of stretch per cycle was equal to the amount of shortening per cycle, and, when isotonic velocity was increased, they could shorten to a lower relative force before this occurred. The modeling thus demonstrates that differences in either cross-bridge cycling rates or myosin light chain kinase activity could potentially underlie the observed relationship between the rate and distance of shortening.

This does not imply, of course, that these are the only possible mechanisms that could account for our observations. There are a number of aspects of ASM that are not included in the model. Perhaps the most notable is the passive viscoelastic properties of the connective tissues, which could contribute to an internal mechanical load opposing shortening. Differences in shortening velocity and amount of shortening could thus have been due to differences in this internal load. The inclusion of passive mechanical elements might also reduce the differences between some of the model predictions and the data. In particular: *1*) it was difficult to reproduce the shape of the observed length-time relationships, and *2*) the model predicted that a 50% increase in force-generating capacity would have an equal or greater influence than a 50% increase in velocity, whereas the opposite was observed experimentally. However, modeling the passive mechanical properties of ASM is nontrivial because these properties are complex and nonlinear, making them difficult to reproduce accurately (3, 8, 45). Our goal in the present study was to determine the extent to which our experimental results could be accounted for solely in terms of cross-bridge kinetics.

To accurately model the isotonic velocity and force-length loops measured in rat trachealis, we had to increase the rate constants for myosin attachment and detachment by 4.5-fold relative to the values used by Mijailovich et al. (30) to model bovine trachealis. While it is not known whether these reaction rates are in fact higher in rat ASM, it seems reasonable that they might be because mass-specific metabolic rate (47) and skeletal muscle intrinsic shortening velocity (34) are both higher in smaller animals.

The length-tension relationships that we used in the model simulations were very different in shape from the isometric length-tension relationship (42) and were inspired by the strong dependence of velocity on length that was observed experimentally (Supplemental Fig. S2). There are a number of reasons why the effective length-tension relationship under dynamic conditions can be expected to differ from the steady-state isometric relationship. First, the observed decrease in shortening velocity with length is thought to be due to the development of an internal load in a structure parallel to the contractile apparatus (21). Because biological soft tissues exhibit stress relaxation (16), such a load is likely to be greatly reduced, or even absent, during isometric contractions. Second, ASM exhibits a phenomenon known as length adaptation, which is characterized by a decrease in isometric force after a length change, followed by a gradual recovery over the next 20–30 min (37). The extent of length adaptation is likely to be different during isometric force-length measurements and active shortening. Third, it has been shown that active shortening itself has a direct depressive effect on the subsequent shortening velocity of ASM (18). Last, intracellular calcium concentration has been shown to decrease as a function of muscle length during active shortening (1).

We also found that to generate behavior similar to that observed during the force oscillation protocol, we would have had to use a different length-tension relationship for each model simulation. This suggests that the dynamic length-tension relationship varies with the loading conditions and muscle properties, which is compatible with the first two mechanisms listed in the preceding paragraph. Specifically, if an internal load is generated by structures that exhibit stress relaxation, this load is expected to be greater when shortening is faster. Similarly, if shortening is faster, then the time available for the muscle to adapt to its current length is decreased. Ideally, rather than using an empirical length-tension relationship to account for the experimentally observed decrease in shortening velocity during the force oscillation protocol, the mechanisms responsible for this behavior would be implemented in the model, thereby allowing the force-length behav-

ior to arise naturally. Unfortunately, we do not yet know enough about the underlying mechanisms for this to be possible.

Fredberg et al. (14) estimated that ASM is stretched by ~12% during the spontaneous sighs that are performed periodically during normal breathing, whereas a maximal deep inspiration from functional residual capacity to total lung capacity would stretch ASM by ~25%. The force oscillations that were used in the present study to simulate deep breaths stretched the muscle by ~8–10% L_{ref} and so were comparable to sighs, rather than maximal deep inspirations. We performed preliminary experiments (data not shown) using larger deep breaths (peak force: 1.53 Fiso) that stretched the muscle strips by 15–20% L_{ref} and seemed to attenuate their ability to shorten so that, after the first deep breath, they often remained at constant length or increased in length. After undergoing this protocol, however, the muscle strips usually did not fully recover, even following a 1- to 1.5-h period of equilibration with electric field stimulation and three MCh stimulations. This suggests that the strips had been irreversibly damaged by the 15–20% stretches, so we chose to use smaller deep breaths for the experiments presented here. It was unexpected that the muscle strips would be damaged by stretch amplitudes that are usually considered to be physiological. This may have been because they were maximally activated, which is likely to be rare in vivo. Maximally activated muscle is very stiff and would probably stretch proportionally less than the surrounding parenchyma during a deep breath (13). Therefore, 25% stretches may not be physiological under conditions of maximal activation. When the force oscillation protocol was performed twice to simulate a change in force-generating capacity, Fiso measured immediately before the two protocols was not significantly different ($P = 0.99$; ratio of isometric force in second/first measurement, means ± SD: 1.01 ± 0.07), indicating complete recovery from the force oscillation protocol when smaller deep breaths were used.

It has been shown that applying length oscillations to activated ASM strips decreases mean muscle force to below isometric force (14, 17, 38, 39) and that applying force oscillations to ASM strips that have been allowed to shorten isotonically causes them to relengthen (15). In the current study, we took a somewhat different approach by applying force oscillations to muscle strips following a period of isometric contraction and studying the subsequent shortening response. An interesting question for future study is whether force oscillations applied in this way reduce the mean shortening velocity relative to an isotonic contraction at the same mean force, as might be expected based on previous studies of the effect of oscillations.

In summary, we have shown that an increase in ASM isotonic velocity is associated with increases in both the rate and the amount of shortening that occurs when the muscle is subjected to an oscillating load, as occurs during breathing. The magnitude of this effect was substantial, being at least comparable to the effect of a proportional increase in the force-generating capacity of the muscle. Therefore, we can conclude that, if ASM velocity is increased in asthma, this could be an important contributor to the associated AHR. We were able to model the increased total amount of shortening with increased isotonic velocity in a cross-bridge model by altering either the cycling rate of the phosphorylated cross-bridges or the rate of myosin light chain phosphorylation. This indicates that an increase in either the content of the +insert myosin isoform or in myosin light chain kinase activity could contribute to AHR. Indeed, it has been shown that mRNA for both of these proteins is elevated in the ASM of asthmatics (28), so increased expression of contractile proteins may explain, at least partially, the AHR observed in asthma.

APPENDIX A: MODEL EQUATIONS AND NUMERICAL INTEGRATION METHOD

The fraction of myosin heads in each of the four states (n_M, n_{Mp}, n_{AMp}, and n_{AM}) varies with both time (t) and x according to four coupled partial differential equations. If we define $\mathrm{N} = [n_M\ n_{Mp}\ n_{AMp}\ n_{AM}]'$, these equations can be written in matrix form as follows:

$$\frac{\partial \mathrm{N}}{\partial t} - v\frac{\partial \mathrm{N}}{\partial x} = \mathrm{RN} \tag{A1}$$

where v is velocity (positive for shortening) and R is a matrix of reaction rates.

$$\mathrm{R} = \begin{bmatrix} -k_1 & k_2 & 0 & g(x) \\ k_1 & -(k_2 + f_p(x)) & g_p(x) & 0 \\ 0 & f_p(x) & -(g_p(x) + k_2) & k_1 \\ 0 & 0 & k_2 & -(g(x) + k_1) \end{bmatrix} \tag{A2}$$

where the rate constants that make up R are defined in the main text. *Equation A1* was solved by treating v as a constant. However, for each time interval, the value of v used was varied so that the force predicted by the model matched the value required for the force oscillation protocol. This process is described in detail in APPENDIX B.

We solved *Eq. A1* using the method of characteristics (49) in Matlab (The Mathworks). This method takes advantage of the fact that, if a myosin head has an initial x-position at $t = 0$ of x_0, then its x-position at time t is given by:

$$x(t) = x_0 - vt \tag{A3}$$

Along the curve (or "characteristic") defined by *Eq. A3*, x_0 and v are constants, so x is a function only of t. Therefore, if the right-hand side of *Eq. A3* is substituted for x in *Eq. A1*, N becomes a function only of t, yielding an ordinary differential equation that can be solved for a given value of x_0. By solving this equation for many different values of x_0, a solution for N can be obtained over the required range of x and t.

We defined characteristics using values of x_0 that were evenly spaced between −9 and 9, at intervals (Δx) of 0.01 and integrated along each characteristic using the trapezoidal method. The time step (Δt) was variable and was calculated as $\Delta t = |\Delta x/v|$ and then adjusted to be a whole fraction of 0.01 s and to have a maximum value of 0.005 s. When x, calculated according to *Eq. A3*, reached −9 during shortening or 9 during stretch, its sign was changed (to 9 or −9, respectively) to allow the characteristics to cover the entire xt space. Any myosin heads that were still attached at this point were forced to detach. Reducing Δx to 0.005 during a simulation of the 20-min force oscillation protocol (described in APPENDIX B) altered the predicted muscle strip length by less than 0.05% L_{ref} throughout the protocol.

Force generated by cross-bridges in the AMp or AM state (F_k, where k indicates the state) was calculated, in arbitrary units, for each time point (t_j) by combining the results obtained for all characteristics as follows:

$$F_k(t_j) = \Delta x \cdot \sum_i x_{ij} \cdot n_k(x_{ij}, t_j) \tag{A4}$$

where x_{ij} is the x-position of characteristic i at time j. Total force was obtained by summing the forces generated by these two states.

APPENDIX B: FORCE CONTROL ALGORITHM USED IN THE MODEL SIMULATIONS

The simulations began with a 6-min period during which length was held constant ($v = 0$). The cross-bridge distribution at the end of this isometric period was used as the initial distribution for simulating the force oscillation protocol and to calculate Fiso using *Eq. A4*. Cross-bridge models usually take velocity as an input and predict force, but to model the force oscillation protocol, we needed to be able to specify force and predict velocity. To do this, we divided the simulation of the 20-min protocol into time intervals of 0.01 s. For each time interval, we proceeded as follows: the model was integrated for 0.01 s beginning with the cross-bridge distributions obtained at the end of the previous time interval and using a velocity that was calculated by linear extrapolation of the velocities used for the previous two time intervals; the force predicted at the end of the 0.01-s simulation was calculated using *Eq. A4*, normalized to Fiso and multiplied by a value between 0 and 1 according to the length-tension relationship that was being used; the absolute difference between the calculated force and the specified target force was determined; if this difference was greater than 0.1% Fiso, the velocity was adjusted according to the algorithm described below and the simulation repeated; this was continued until the predicted force was within 0.1% Fiso of the target force, and then the next time interval was simulated. The velocity adjustment was performed by changing the velocity by an amount that was proportional to the error between the predicted force and the target force. The constant of proportionality was changed at each iteration as follows: it was increased if the previous velocity adjustment had decreased the force error by less than 50%, it was decreased if the previous adjustment had resulted in a change in the sign of the error (indicating an overshoot of the target value), and it was multiplied by -1 if the previous adjustment had increased the magnitude of the error. This approach was found to give a closer correspondence between the actual force and target force than a feedback control method used previously (7).

ACKNOWLEDGMENTS

We thank Amanda Elvin for advice on numerical integration methods and Linda Kachmar for technical assistance.

GRANTS

The authors of this work were supported by National Heart, Lung, and Blood Institute Grants HL-87791, HL-87788, HL-87401, and HL-67273, the Canadian Institutes for Health Research (MOP-7954), and the Royal Society of New Zealand. The Meakins-Christie Laboratories are supported in part by a center grant from Le Fonds de la Recherche en Santé du Québec and by the J. T. Costello Memorial Research Fund.

DISCLOSURES

No conflicts of interest, financial or otherwise, are declared by the author(s).

REFERENCES

1. **An SS, Hai CM.** Mechanical signals and mechanosensitive modulation of intracellular [Ca^{2+}] in smooth muscle. *Am J Physiol Cell Physiol* 279: C1375–C1384, 2000.
2. **Antonissen LA, Mitchell RW, Kroeger EA, Kepron W, Tse KS, Stephens NL.** Mechanical alterations of airway smooth muscle in a canine asthmatic model. *J Appl Physiol* 46: 681–687, 1979.
3. **Bates JHT.** A recruitment model of quasi-linear power-law stress adaptation in lung tissue. *Ann Biomed Eng* 35: 1165–1174, 2007.
4. **Bates JHT, Bullimore SR, Politi AZ, Sneyd J, Anafi RC, Lauzon AM.** Transient oscillatory force-length behavior of activated airway smooth muscle. *Am J Physiol Lung Cell Mol Physiol* 297: L362–L372, 2009.
5. **Berend N, Salome CM, King GG.** Mechanisms of airway hyperresponsiveness in asthma. *Respirology* 13: 624–631, 2008.
6. **Blanc FX, Coirault C, Salmeron S, Chemla D, Lecarpentier Y.** Mechanics and crossbridge kinetics of tracheal smooth muscle in two inbred rat strains. *Eur Respir J* 22: 227–234, 2003.
7. **Bullimore SR, Saunders TJ, Herzog W, MacIntosh BR.** Calculation of muscle maximal shortening velocity by extrapolation of the force-velocity relationship: afterloaded versus isotonic release contractions. *Can J Physiol Pharmacol* 88: 937–948, 2010.
8. **Donovan GM, Bullimore SR, Elvin AJ, Tawhai MH, Bates JHT, Lauzon AM, Sneyd J.** A continuous-binding crosslinker model for passive airway smooth muscle. *Biophys J*. In press.
9. **Duguet A, Biyah K, Minshall E, Gomes R, Wang CG, Taoudi-Benchekroun M, Bates JHT, Eidelman DH.** Bronchial responsiveness among inbred mouse strains: role of airway smooth-muscle shortening velocity. *Am J Respir Crit Care Med* 161: 839–848, 2000.
10. **Duracher C, Blanc FX, Gueugniaud PY, David JS, Riou B, Lecarpentier Y, Coirault C.** The effects of isoflurane on airway smooth muscle crossbridge kinetics in Fisher and Lewis rats. *Anesth Analg* 101: 136–142, 2005.
11. **Fan T, Yang M, Halayko A, Mohapatra SS, Stephens NL.** Airway responsiveness in two inbred strains of mouse disparate in IgE and IL-4 production. *Am J Respir Cell Mol Biol* 17: 156–163, 1997.
12. **Florio C, Styhler A, Heisler S, Martin JG.** Mechanical responses of tracheal tissue in vitro: dependance on the tissue preparation employed and relationship to smooth muscle content. *Pulm Pharmacol* 9: 157–166, 1996.
13. **Fredberg JJ.** Frozen objects: small airways, big breaths, asthma. *J Allergy Clin Immunol* 106: 615–624, 2000.
14. **Fredberg JJ, Inouye D, Miller B, Nathan M, Jafari S, Raboudi SH, Butler JP, Shore SA.** Airway smooth muscle, tidal stretches, and dynamically determined contractile states. *Am J Respir Crit Care Med* 156: 1752–1759, 1997.
15. **Fredberg JJ, Inouye DS, Mijailovich SM, Butler JP.** Perturbed equilibrium of myosin binding in airway smooth muscle and its implications in bronchospasm. *Am J Respir Crit Care Med* 159: 959–967, 1999.
16. **Fung YC.** *Biomechanics: mechanical properties of living tissues* (2nd edition). New York: Springer-Verlag, 1993.
17. **Gunst SJ.** Contractile force of canine airway smooth muscle during cyclical length changes. *J Appl Physiol* 55: 759–769, 1983.
18. **Gunst SJ, Wu MF, Smith DD.** Contraction history modulates isotonic shortening velocity in smooth muscle. *Am J Physiol Cell Physiol* 265: C467–C476, 1993.
19. **Hai CM, Murphy RA.** Cross-bridge phosphorylation and regulation of latch state in smooth muscle. *Am J Physiol Cell Physiol* 254: C99–C106, 1988.
20. **Hai CM, Murphy RA.** Regulation of shortening velocity by cross-bridge phosphorylation in smooth muscle. *Am J Physiol Cell Physiol* 255: C86–C94, 1988.
21. **Harris DE, Warshaw DM.** Slowing of velocity during isotonic shortening in single isolated smooth muscle cells: evidence for an internal load. *J Gen Physiol* 96: 581–601, 1990.
22. **Huxley AF.** Muscle structure and theories of contraction. *Prog Biophys Biophys Chem* 7: 255–318, 1957.
23. **Jackson AC, Murphy MM, Rassulo J, Celli BR, Ingram RH.** Deep breath reversal and exponential return of methacholine-induced obstruction in asthmatic and nonasthmatic subjects. *J Appl Physiol* 96: 137–142, 2004.
24. **Jeffery PK.** Remodeling in asthma and chronic obstructive lung disease. *Am J Respir Crit Care Med* 164: S28–S38, 2001.
25. **Jensen A, Atileh H, Suki B, Ingenito EP, Lutchen KR.** Airway caliber in healthy and asthmatic subjects: effects of bronchial challenge and deep inspirations. *J Appl Physiol* 91: 506–515, 2001.
26. **Lambert RK, Wiggs BR, Kuwano K, Hogg JC, Pare PD.** Functional significance of increased airway smooth muscle in asthma and COPD. *J Appl Physiol* 74: 2771–2781, 1993.
27. **Lauzon AM, Tyska MJ, Rovner AS, Freyzon Y, Warshaw DM, Trybus KM.** A 7-amino-acid insert in the heavy chain nucleotide binding loop alters the kinetics of smooth muscle myosin in the laser trap. *J Muscle Res Cell Motil* 19: 825–837, 1998.
28. **Leguillette R, Laviolette M, Bergeron C, Zitouni N, Kogut P, Solway J, Kachmar L, Hamid Q, Lauzon AM.** Myosin, transgelin, and myosin light chain kinase expression and function in asthma. *Am J Respir Crit Care Med* 179: 194–204, 2009.
29. **Ma X, Cheng Z, Kong H, Wang Y, Unruh H, Stephens NL, Laviolette M.** Changes in biophysical and biochemical properties of single bronchial smooth muscle cells from asthmatic subjects. *Am J Physiol Lung Cell Mol Physiol* 283: L1181–L1189, 2002.
30. **Mijailovich SM, Butler JP, Fredberg JJ.** Perturbed equilibria of myosin binding in airway smooth muscle: bond-length distributions, mechanics, and ATP metabolism. *Biophys J* 79: 2667–2681, 2000.

31. **Mitchell RW, Ndukwu IM, Arbetter K, Solway J, Leff AR.** Effect of airway inflammation on smooth muscle shortening and contractility in guinea-pig trachealis. *Am J Physiol Lung Cell Mol Physiol* 265: L549–L554, 1993.
32. **Mitchell RW, Ruhlmann E, Magnussen H, Leff AR, Rabe KF.** Passive sensitization of human bronchi augments smooth muscle shortening velocity and capacity. *Am J Physiol Lung Cell Mol Physiol* 267: L218–L222, 1994.
33. **Oliver MN, Fabry B, Marinkovic A, Mijailovich SM, Butler JP, Fredberg JJ.** Airway hyperresponsiveness, remodeling, and smooth muscle mass: right answer, wrong reason? *Am J Respir Cell Mol Biol* 37: 264–272, 2007.
34. **Pellegrino MA, Canepari M, Rossi R, D'Antona G, Reggiani C, Bottinelli R.** Orthologous myosin isoforms and scaling of shortening velocity with body size in mouse, rat, rabbit and human muscles. *J Physiol* 546: 677–689, 2003.
35. **Pellegrino R, Wilson O, Jenouri G, Rodarte JR.** Lung mechanics during induced bronchoconstriction. *J Appl Physiol* 81: 964–975, 1996.
36. **Piazzesi G, Lombardi V.** A cross-bridge model that is able to explain mechanical and energetic properties of shortening muscle. *Biophys J* 68: 1966–1979, 1995.
37. **Pratusevich VR, Seow CY, Ford LE.** Plasticity in canine airway smooth muscle. *J Gen Physiol* 105: 73–94, 1995.
38. **Shen X, Wu MF, Tepper RS, Gunst SJ.** Mechanisms for the mechanical response of airway smooth muscle to length oscillation. *J Appl Physiol* 83: 731–738, 1997.
39. **Shen X, Wu MF, Tepper RS, Gunst SJ.** Pharmacological modulation of the mechanical response of airway smooth muscle to length oscillation. *J Appl Physiol* 83: 739–745, 1997.
40. **Siddiqui S, Jo T, Tamaoka M, Shalaby KH, Ghezzo H, Bernabeu M, Martin JG.** Sites of allergic airway smooth muscle remodeling and hyperresponsiveness are not associated in the rat. *J Appl Physiol* 109: 1170–1178, 2010.
41. **Solway J, Fredberg JJ.** Perhaps airway smooth muscle dysfunction contributes to asthmatic bronchial hyperresponsiveness after all. *Am J Respir Cell Mol Biol* 17: 144–146, 1997.
42. **Stephens NL, Kroeger E, Mehta JA.** Force-velocity characteristics of respiratory airway smooth muscle. *J Appl Physiol* 26: 685–692, 1969.
43. **Stephens NL, Morgan G, Kepron W, Seow CY.** Changes in cross-bridge properties of sensitized airway smooth muscle. *J Appl Physiol* 61: 1492–1498, 1986.
44. **Tao FC, Tolloczko B, Eidelman DH, Martin JG.** Enhanced Ca^{2+} mobilization in airway smooth muscle contributes to airway hyperresponsiveness in an inbred strain of rat. *Am J Respir Crit Care Med* 160: 446–453, 1999.
45. **Trepat X, Deng LH, An SS, Navajas D, Tschumperlin DJ, Gerthoffer WT, Butler JP, Fredberg JJ.** Universal physical responses to stretch in the living cell. *Nature* 447: 592–596, 2007.
46. **Wang CG, Almirall JJ, Dolman CS, Dandurand RJ, Eidelman DH.** In vitro bronchial responsiveness in two highly inbred rat strains. *J Appl Physiol* 82: 1445–1452, 1997.
47. **West GB, Woodruff WH, Brown JH.** Allometric scaling of metabolic rate from molecules and mitochondria to cells and mammals. *Proc Natl Acad Sci USA* 99: 2473–2478, 2002.
48. **Yu SN, Crago PE, Chiel HJ.** A nonisometric kinetic model for smooth muscle. *Am J Physiol Cell Physiol* 272: C1025–C1039, 1997.
49. **Zahalak GI.** A distribution moment approximation for kinetic theories of muscular contraction. *Math Biosci* 55: 89–114, 1981.